

## Enzymatically Synthesized Conducting Polyaniline Nanocomposites: A Solid-State NMR Study

Muthiah Thiyagarajan,<sup>1</sup> Jayant Kumar,<sup>1</sup> Lynne A. Samuelson,<sup>2</sup>  
and Ashok L. Cholli<sup>1,\*</sup>

<sup>1</sup>Center for Advanced Materials, University of Massachusetts—Lowell,  
Lowell, Massachusetts, USA

<sup>2</sup>Natick Soldier Center, U.S. Army RDECOM, Natick, Massachusetts, USA

### ABSTRACT

The chiral conducting polyaniline (PANI) nanocomposites [polyacrylic acid/polyaniline/(–) camphorsulphonic acid (CSA)] were synthesized using enzyme, horseradish peroxidase (HRP) in the aqueous buffer solution at pH 4.3. It appears that the enzyme HRP apart being a biocatalyst, plays an important role during the polymerization, which allows PANI to prefer a specific helical conformation whether the induced chirality in the monomer-CSA complex is either by (+)CSA or (–)CSA. In this paper, we report, the structural characterization of these nanocomposites by solid-state <sup>13</sup>C cross-polarization with magic angle spinning (CP/MAS) NMR techniques. The structural features of PANI in the conducting form of nanocomposite (as-synthesized) are similar to that of enzymatically and chemically synthesized PANI. Preliminary data also suggest that some portion of nanocomposite samples are not completely doped. Dedoping of as-synthesized PANI nanocomposite with aqueous NH<sub>4</sub>OH shows the spectral features that of the emeraldine base form. Solid-state <sup>13</sup>C NMR data suggest that it is possible to detach PAA and CSA from PANI in the nanocomposite material.

*Key Words:* Solid-state <sup>13</sup>C NMR CP/MAS NMR: Conducting polyaniline; Nanocomposites; Enzymatic polymerization.

## INTRODUCTION

Among conducting polymers, polyaniline (PANI) has significant importance because of its ease of processibility, good environmental stability, and high conductivity.<sup>[1]</sup> Conductivity exhibits a strong dependence on solution pH<sup>[2]</sup> and oxidation state.<sup>[3]</sup> Young et al. studied the oxidation state of PANI film processed in the presence of gel inhibitor, the extent of reactivity and changes in the morphology and chain dynamics using <sup>13</sup>C and <sup>15</sup>N solid-state NMR.<sup>[4]</sup> The chiral conducting PANI nanocomposites have been synthesized by chemical<sup>[5,6]</sup> and electrochemical methods.<sup>[7]</sup> Wehrli et al.<sup>[8]</sup> observed the excessive line broadening of the <sup>15</sup>N resonance peaks in the solid-state NMR spectrum as a result of higher conductivities in the chemically synthesized PANI. Recently, a novel and environmentally friendly enzymatic approach has been developed to synthesize water-soluble conducting PANI in the presence of various templates.<sup>[9,10]</sup> This method has been extended to synthesize optically active conducting PANI nanocomposites<sup>[11]</sup> in the presence of H<sub>2</sub>O<sub>2</sub> as an oxidant, using (+) and (-)10-camphorsulfonic acid (CSA) as a dopant and chiral inductor. The formation of chiral PANI in the nanocomposites was confirmed by circular dichroism (CD). Interestingly, the CD spectra of nanocomposites formed either with (+) or (-)CSA show the enzyme, horseradish peroxidase (HRP) not only acts as a biocatalyst but itself plays a critical role in controlling the stereo specificity of the PANI in the nanocomposite. It was shown that enzyme (HRP) regulates the helical conformation to a specific handedness for the PANI chains during polymerization, regardless whether induced chirality in the complex CSA-aniline is from (+) or (-)CSA. UV-VIS spectra show that the PANI is in the conducting form and transmission electron micrographs (TEM) show that the nanocomposites are dispersed nicely with particle size dimensions in the range of 20–50 nm. Electron diffraction patterns of these chiral polymer nanocomposites suggest that these nanocomposites exist in both crystalline and amorphous states. In this paper, we report the structural characterization of enzymatically synthesized PANI nanocomposites using solid-state <sup>13</sup>C cross-polarization with magic angle spinning (CP/MAS) NMR experiments. The solid-state NMR spectral features of PANI nanocomposites are also compared with chemically and enzymatically synthesized PANI in their doped and dedoped states.

## EXPERIMENTAL

### Enzymatic Synthesis of Polyaniline Nanocomposites

In a typical procedure, aniline/polyacrylic acid (1:1 molar ratio) was added to a 10 mL of 0.01 M sodium phosphate buffer. Molecular weight of PAA is 250,000. The reaction solution was stirred for 6 h to ensure a complete adduct formation. To this adduct solution, 0.6 mL of 2 M (-)CSA was added. Then, pH of the solution was adjusted to pH 4.3. A solution of HRP (3 mg in 0.5 mL) was then added and continuously stirred. The reaction was then initiated with an incremental addition of hydrogen peroxide (H<sub>2</sub>O<sub>2</sub>). To avoid the inhibition of HRP due to excess of H<sub>2</sub>O<sub>2</sub>, a 5% solution of H<sub>2</sub>O<sub>2</sub> (20 aliquots of 25  $\mu$ L each) was added drop wise with a time interval of 3 min between each addition. The reaction mixture was stirred for 1 h after which a dark green PAA/PANI/(-)CSA complex precipitated out of solution. The PAA/PANI/(-)CSA complex was filtered and washed

with acetone and water to remove unreacted monomer and dried under vacuum. The dedoping was carried out using aqueous  $\text{NH}_4\text{OH}$ . The conductivity measurements were made using a Cascade Microtech four-point probe and showed low conductivity ( $1.8 \times 10^{-2} \text{ S cm}^{-1}$ ) for the PANI nanocomposite sample.

### Solid-State NMR Measurements

Solid-state  $^{13}\text{C}$  NMR experiments were performed on a 300 MHz Bruker DMX 7.05 Tesla widebore magnet with a 4 mm triple resonance broad band probe head. Zirconium oxide ( $\text{ZrO}_2$ ) 4 mm (o.d.) rotor was used with Kel-F caps for all measurements. A one-time magic angle adjustment was accomplished by maximizing the spinning side band intensities of  $^{79}\text{Br}$  NMR signal of the KBr sample. All the spectra were recorded at room temperature using a rotor spinning speed of 10 kHz. The typical parameters for  $^{13}\text{C}$  CP/MAS NMR experiments were as follows: spin lock and decoupling field of 70 kHz, 3 s recycle time, contact time varied from 100  $\mu\text{s}$  to 10 ms and sweep width of 31 kHz. The total number of free induction decays (FIDs) co-added per spectrum is 20,000 and processed by exponential apodization function with a line broadening of 50 Hz. All the  $^{13}\text{C}$  CP/MAS NMR spectra were externally referenced to glycine by assigning the carbonyl signal at 176.3 ppm with respect to tetramethylsilane (TMS).

### RESULTS AND DISCUSSION

The solid-state  $^{13}\text{C}$  CP/MAS NMR spectra of enzymatically synthesized, self-doped PAA/PANI/(-)CSA nanocomposites are shown in Fig. 1(c)–(e) with contact times ranging from 50 to 700  $\mu\text{s}$ . Two broad resonances are observed, one in the upfield region of 10–70 ppm for aliphatic carbons of PAA, (-)CSA and other one for aromatic carbon resonances of PANI (100–170 ppm). A broad peak, as expected, is observed in Fig. 1 for PANI resonances 100–170 ppm region. The line width of the  $^{13}\text{C}$  resonance peak of conducting PANI is ca. 25 ppm whereas chemically synthesized conducting PANI is ca. 60.0 ppm.<sup>[3,12]</sup> A broad resonance centered about 128.5 ppm for conducting PANI in the nanocomposites. The line broadening for the resonance peak of conducting PANI is attributed to the site heterogeneity and a distribution of isotropic chemical shifts.<sup>[13]</sup> Solid-state  $^{13}\text{C}$  CP/MAS NMR spectra of (-)CSA and PAA are also presented in Fig. 1(a) and (b) with a contact time of 150  $\mu\text{s}$ . The peaks at 217.8 ppm in spectrum "a" and 181.7 ppm in spectrum "b" are assigned to carbonyl carbon resonances of (-)CSA and PAA, respectively. These carbonyl resonance peaks are also observed in the  $^{13}\text{C}$  NMR spectra of nanocomposites (spectra c–e). As the contact time was increased from 50 to 700  $\mu\text{s}$ , the intensity of the non-protonated carbon resonances of PANI is also increased [Fig. 1(c–e)]. As a result, an unresolved shoulder appears at ca. 140–170 ppm for aromatic carbons of PANI. Similarly, the intensity of carbonyl carbon resonance of (-)CSA at 217.8 ppm, PAA at 181.7 ppm and quaternary carbon resonances of (-)CSA (51.2, 58.5 ppm) [Fig. 1(e)] are also enhanced in the spectra of nanocomposites. It is very unusual to observe a shoulder peak at 125.7 ppm in the  $^{13}\text{C}$  NMR spectrum of conducting PANI sample. Normally a broad featureless resonance peak is observed for conducting PANI whether it is chemically<sup>[3]</sup> or enzymatically synthesized.<sup>[14]</sup> It was observed that the peak position of

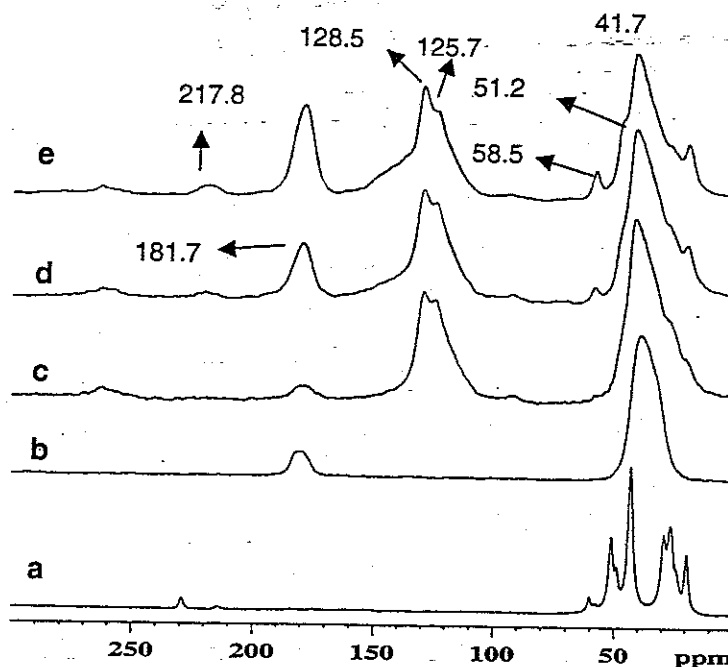


**Figure 1.** Solid-state  $^{13}\text{C}$  CP/MAS NMR spectra of (a) (-)CSA, contact time  $150\ \mu\text{s}$ ; (b) PAA, contact time  $150\ \mu\text{s}$ ; and (c)–(e) enzymatically synthesized self-doped conducting form PANI nanocomposites (PAA/PANI/(-)CSA) with contact time of 50, 300, and  $700\ \mu\text{s}$ , respectively.

this broad peak shifts to an upfield by ca. 5 ppm in the base form of PANI.<sup>[15]</sup> The presence of a shoulder in the spectra (c)–(e) and a broad downfield shoulder in the 130–170 ppm region in Fig. 1 may be due to the presence of non-conducting PANI domains in the PANI nanocomposite sample. The presence of non-conducting regions in the nanocomposites may explain the low conductivity for these materials ( $\sigma = \sim 10^{-6}\ \text{S/cm}$ ).

Figure 2 shows the solid-state  $^{13}\text{C}$  CP/MAS NMR spectra of PANI nanocomposites (PAA/PANI/(-)CSA) in both doped (spectrum "a") and dedoped forms (spectrum "b"). The broad peaks at ca. 110–140 ppm are assigned to benzenoid carbon resonances of PANI in its doped form [Fig. 2(a), contact time  $300\ \mu\text{s}$ ]. As discussed above, the solid-state NMR spectrum of nanocomposites show the resonance for the carbonyl group at 181.7 ppm and a broad resonance peak ca. 10–60 ppm for aliphatic carbons of PAA and CSA. The aliphatic carbon resonances for CSA are superimposed on the aliphatic resonances of PAA. The dedoped base form of PANI nanocomposites [Fig. 2(b), without dipolar dephasing] shows peaks at ca. 140–170 ppm which are due to non-protonated carbon resonances of benzenoid and quinoid rings. The aliphatic carbon resonances of PAA and CSA are significantly reduced as a result of the dedoping process [Fig. 2(b)] and only the residual amount of PAA and CSA are present in the sample. This suggests that it is possible to remove template and chiral acid by the process of dedoping. The dipolar dephasing  $^{13}\text{C}$  CP/MAS NMR spectra with a dephasing delay of  $30\ \mu\text{s}$  are shown in spectrum "c" with a CP contact time of 6 ms and spectrum "d" with a CP contact time of 8 ms. This technique is normally used to suppress the magnetization due to protonated aromatic carbons,

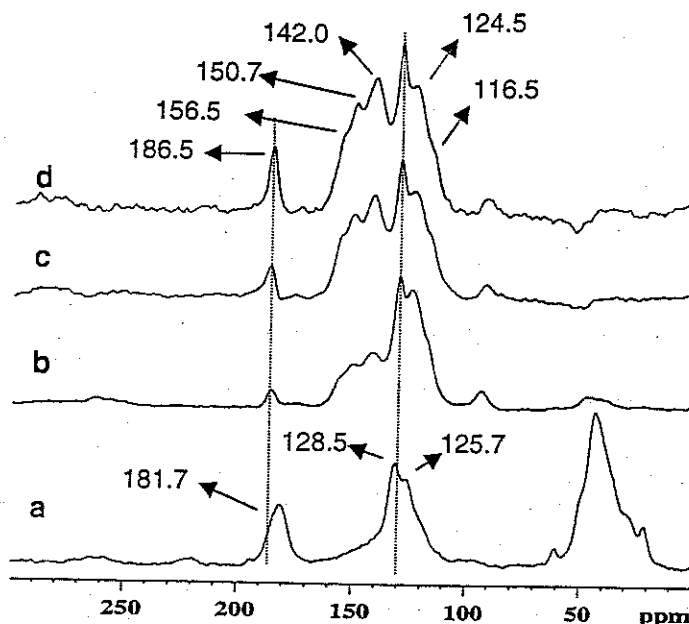


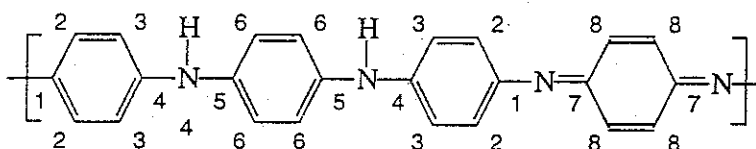
**Figure 2.** Solid-state  $^{13}\text{C}$  CP/MAS NMR spectra of PANI nanocomposites (PAA/PANI/(–)CSA: (a) self-doped conducting form of PANI, contact time 300  $\mu\text{s}$ ; (b) dedoped base form of PANI, contact time 10 ms; (c) dedoped base form of PANI, contact time 6 ms with dipolar dephasing delay of 30  $\mu\text{s}$ ; and (d) dedoped base form of PANI, contact time 8 ms with dipolar dephasing delay of 30  $\mu\text{s}$ .

thereby enhancing the non-protonated aromatic carbon resonances of PANI. The peaks at 142.0 (C-4 and C-5) and 150.7 ppm (C-1) are assigned to benzenoid amine carbon resonances of PANI. The peak at 156.5 ppm (C-7) is assigned to imine quinoid carbon resonances of PANI in the base form. The peaks at 124.5 ppm (C-2 and C-3) and 116.5 ppm (C-6) are assigned to protonated aromatic benzenoid carbons of PANI. The peak at 128.5 ppm (C-8) is assigned to quinoid carbon of PANI. The presence of down-field resonance at 186.5 ppm may be due to oxidation of the PANI chain ends to form  $\text{N}=\text{O}$ , which shifts the neighboring non-protonated aromatic carbon resonance. Solid-state NMR analysis of the base form of nanocomposites suggests the presence of benzenoid-quinoid type structures of emeraldine PANI in the base form. The  $^{13}\text{C}$  chemical shift assignments of PANI nanocomposites in the dedoped form are given in Table 1.

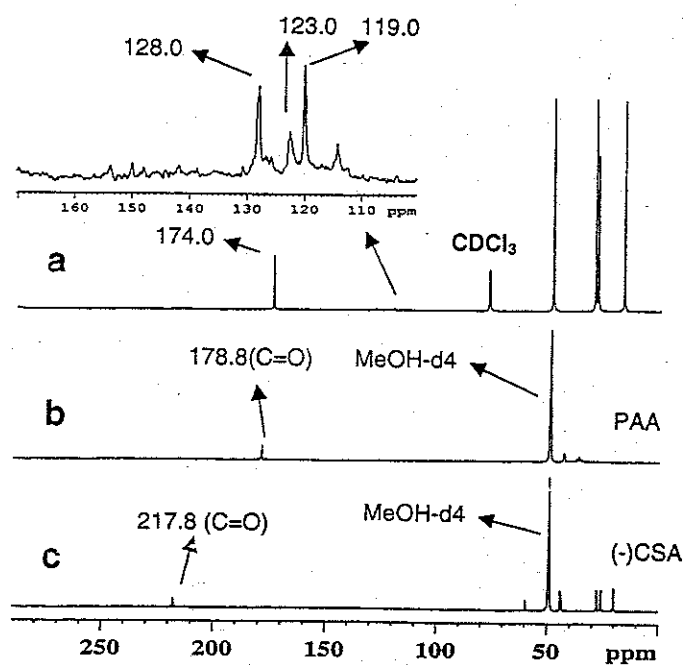
To confirm the absence of template and CSA as a result of dedoping process, solution  $^{13}\text{C}$  NMR spectrum was recorded of PANI dissolved in NMP solvent using  $\text{CDCl}_3$  [Fig. 3(a)]. The benzenoid protonated carbon resonances of PANI appear in the region of 110–130 ppm. The peaks at 119.0 (C-6), 123.0 ppm (C-3 and C-3) are assigned to benzenoid protonated carbon resonances of PANI [Inset Fig. 3(a)]. The peak at 128.0 ppm (C-8) is assigned to quinoid carbon resonance and the weak resonances due to amine and imine non-protonated quaternary carbon resonances of PANI also appear at ca. 140–160 ppm. The peak at 178.8 ppm [Fig. 3(b)] and 217.8 ppm [Fig. 3(c)] were assigned to the carbonyl carbon resonances of CSA and PAA, respectively. The corresponding  $^{13}\text{C}$  solution NMR spectra of PANI nanocomposites in aliphatic region are shown in Fig. 4. A resonance peak

**Table 1.**  $^{13}\text{C}$  CP/MAS NMR chemical shifts of PANI nanocomposites.

Carbon number	Base form of PANI, chemical shifts (ppm)		
	Nanocomposite base form	Chemically synthesized PANI [3]	Enzymatically synthesized PANI [12]
1	150.7	146.7	145.0
2	124.5	123.6	123.0
3	124.5	123.6	123.0
4	142.0	141.6	140.0
5	142.0	141.6	140.0
6	116.5	117.0	114.0
7	156.5	156.8	157.0
8	128.5	135.2	136.0



Dedoped base form of PANI obtained from nanocomposites

**Figure 3.** Solution  $^{13}\text{C}$  NMR spectra of (a) (-)-CSA, using  $\text{MeOH-d}_4$ ; (b) PAA, using  $\text{MeOH-d}_4$ ; and (c) dedoped base form of PANI nanocomposites (PAA/PANI/(-)-CSA) in NMP solvent, using  $\text{CDCl}_3$ .

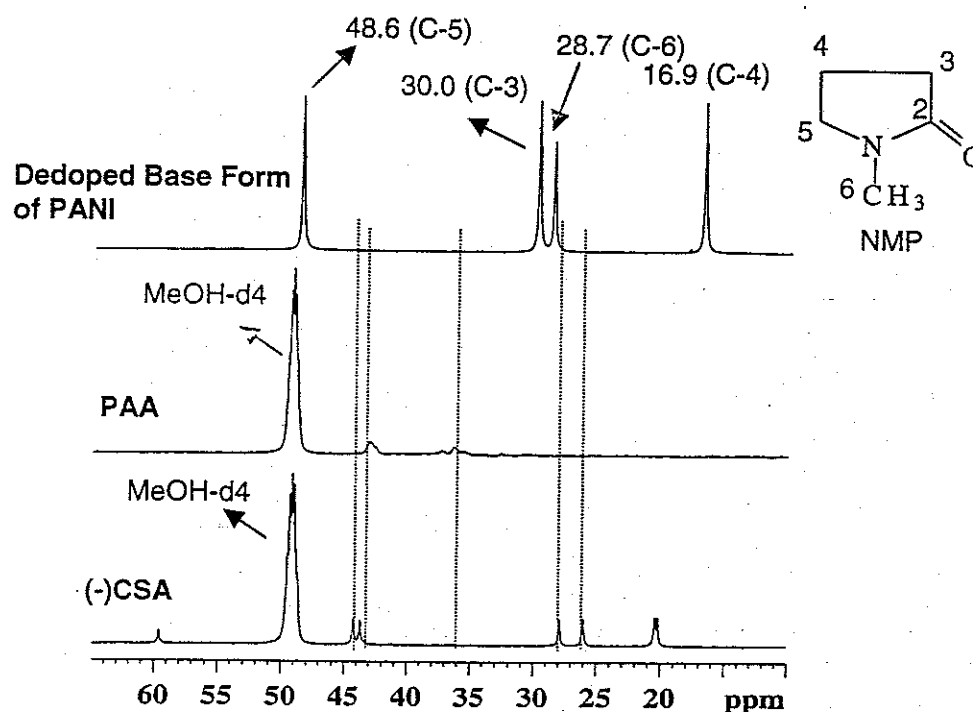


Figure 4. The corresponding  $^{13}\text{C}$  NMR spectra of (a)  $(-)\text{CSA}$ , using  $\text{MeOH-d}_4$ ; (b) PAA, using  $\text{MeOH-d}_4$ ; and (c) dedoped base form of PANI nanocomposites in aliphatic region.

at 28.7 ppm is assigned to methyl carbon. The peaks at 16.9, 30.0, and 48.6 ppm are assigned to methylene carbon resonances of the NMP solvent. The aliphatic carbon resonances of the template and chiral acid are not observed in the spectrum of dedoped PANI nanocomposite (top spectrum in Fig. 4). This result suggests the absence of template and CSA after subjecting the conducting PANI composite sample to the dedoping process.

Figure 5 shows the infrared spectra of self doped PAA/PANI/ $(-)\text{CSA}$  nanocomposites, PAA, and  $(-)\text{CSA}$ . FT-IR spectrum of PAA/PANI/ $(-)\text{CSA}$  nanocomposites [Fig. 5 (a)] shows vibration bands at ca. 1600 and 1500  $\text{cm}^{-1}$  which are due to quinoid and benzenoid ring deformation, respectively. The absorption band ca. 780  $\text{cm}^{-1}$  is due to 1,4 substituted phenyl rings. The peak appearing at ca. 3500  $\text{cm}^{-1}$  is assigned to the N—H vibration and hydroxyl stretching of PAA. The band appearing at 1050  $\text{cm}^{-1}$  is due to asymmetric and symmetric stretching of  $\text{SO}_3^-$ , indicating the presence of  $(-)\text{CSA}$  in the sample. The presence of  $(-)\text{CSA}$  as dopant and PAA as template in the PANI nanocomposites is further confirmed by a strong —C—H vibration band appearing at around 2950  $\text{cm}^{-1}$ . The intense broad peak at around 1710  $\text{cm}^{-1}$  has been assigned to the carbonyl stretching of  $(-)\text{CSA}$  and PAA, in Fig. 5 (c) and (d). There is no peak observed for the carbonyl stretching of PAA and  $(-)\text{CSA}$  in the dedoped base form of PANI nanocomposites [Fig. 5 (b)]. This result confirms the removal of PAA and  $(-)\text{CSA}$  during dedoping using dilute  $\text{NH}_4\text{OH}$ .

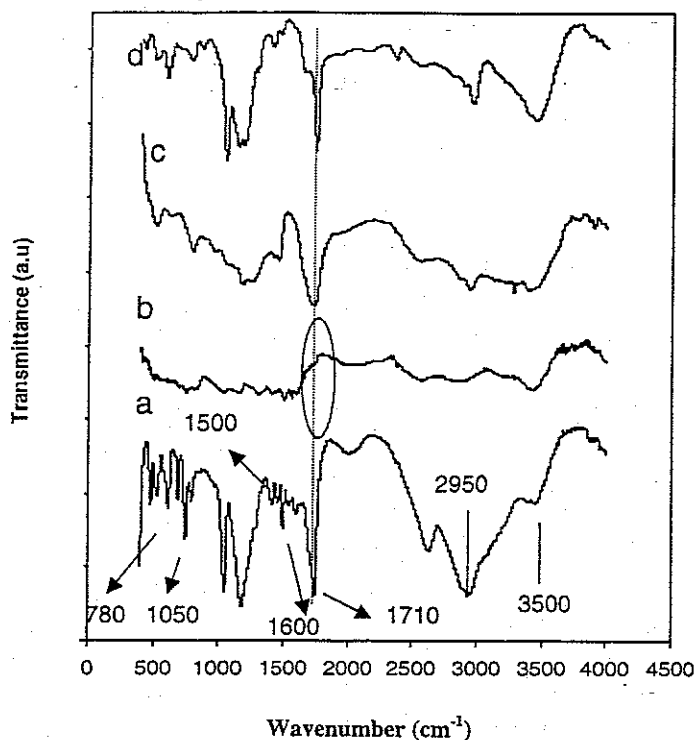


Figure 5. FT-IR spectra of (a) self-doped conducting form of PANI nanocomposites (PAA/PANI/(-)CSA); (b) dedoped base form of PANI nanocomposites (PAA/PANI/(-)CSA); (c) PAA; and (d) (-)CSA.

## CONCLUSION

The structural features of the conducting and base forms of enzymatically synthesized PANI nanocomposites have been studied by solid-state NMR techniques. These results are similar to that of chemically and enzymatically synthesized PANI. Solid-state and solution NMR and IR data suggest that the template (PAA) and (-)CSA were removed upon dedoping using  $\text{NH}_4\text{OH}$ . The low conductivity measurement of these samples is probably related to structural variations in the as-synthesized conducting nanocomposites. The solid state  $^{13}\text{C}$  NMR data on as-synthesized PANI suggest that there are non-conducting domains present in the sample. This may explain the low conductivity of the sample.

## ACKNOWLEDGMENTS

The authors thank the National Science Foundation for a research grant (Grant #DMR-9986644). We thank Dr. Ramaswamy Nagarajan for conductivity measurement, Mr. Xiadong Wu and Mr. Jeff Njus for helpful discussions. This work is dedicated to memory of the late Professor S. K. Tripathy.

## REFERENCES

1. Hiromasa, G.; Akagi, K. Synthesis and properties of polyaniline derivatives with liquid crystallinity. *Macromolecules* **2002**, *35*, 2545–2551.
2. Chiang, J.C.; MacDiarmid, A.G. "Polyaniline": protonic acid doping of the emeraldine form to the metallic regime. *Synth. Met.* **1986**, *13*, 193–205.
3. Kaplan, S.; Conwell, E.M.; Richter, A.F.; MacDiarmid, A.G. Solid state  $^{13}\text{C}$  NMR characterization of polyanilines. *J. Am. Chem. Soc.* **1988**, *110*, 7647–7651.
4. Young, T.L.; Espe, M.P.; Yang, D.; Mattes, B.R. Application of solid-state NMR to characterize the interaction of gel inhibitors with emeraldine base polyaniline. *Macromolecules* **2002**, *35*, 5565–5569.
5. McCarthy, P.A.; Huang, J.; Yang, S.C.; Wang, H.L. Synthesis and characterization of water soluble chiral conducting polymer nanocomposites. *Langmuir* **2002**, *18*, 259–263.
6. Li, W.; Liu, D.; McCarthy, P.A.; Huang, J.; Yang, S.; Wang, H.L. Towards understanding and optimizing the template-guided synthesis of chiral polyaniline nanocomposites. *Macromolecules* **2002**, *35*, 9975.
7. Innis, P.C.; Norris, I.D.; Kane-Maguire, L.A.P.; Wallace, G.G. Electrochemical formation of chiral polyaniline colloids codoped with (+) or (–)-10-camporsulfonic acid and polystyrene sulfonate. *Macromolecules* **1998**, *31*, 6521–6528.
8. Wherl, B.; Limbach, H.-H.; Mortensen, J.; Heinze, J.  $^{15}\text{N}$  CP MAS NMR Study of the structure of polyaniline. *Angew. Chem. Int. Ed. Engl. Adv. Mater.* **1989**, *28*, 1741–1743.
9. Liu, W.; Kumar, J.; Tripathy, S.; Senecal, K.J.; Samuelson, L. Enzymatically synthesized conducting polyaniline. *J. Am. Chem. Soc.* **1999**, *121*, 71–78.
10. Liu, W.; Cholli, A.L.; Nagarajan, R.; Kumar, J.; Tripathy, S.; Bruno, F.F.; Samuelson, L. The role of template in the enzymatic synthesis of conducting polyaniline. *J. Am. Chem. Soc.* **1999**, *121*, 11345–11355.
11. Thiagarajan, M.; Samuelson, L.; Kumar, J.; Cholli, A.L. Helical conformational specificity of enzymatically synthesized chiral conducting polyaniline nanocomposites. *J. Am. Chem. Soc.* **2003** (Communicated).
12. Kabaya, S.; Appel, M.; Haba, Y.; Titleman, G.L.; Schmidt, A. Polyaniline dodecylbenzene sulphonic acid polymerized from aqueous medium: a solid-state NMR characterization. *Macromolecules* **1999**, *32*, 5357–5364.
13. Espe, M.P.; Mattes, B.R.; Schaefer, J. Packing in amorphous regions of hydrofluoric acid doped polyaniline powder by  $^{15}\text{N}$ - $^{19}\text{F}$  REDOR NMR. *Macromolecules* **1997**, *30*, 6307.
14. Sahoo, S.K.; Nagarajan, R.; Samuelson, L.; Kumar, J.; Cholli, A.L.; Tripathy, S.K. Enzymatically synthesized polyaniline in presence of template poly(vinyl phosphonic acid): a solid-state NMR study. *J. Macromol. Sci. Part A: Pure and Appl. Chem.* **2001**, *38* (12), 1315–1328.
15. Sahoo, S.K.; Nagarajan, R.; Chakraborty, S.; Samuelson, L.; Kumar, J.; Cholli, A.L. Variation in the structure of conducting polyaniline with and without the presence of template during enzymatic polymerization: a solid-state NMR study. *J. Macromol. Sci. Part A: Pure and Appl. Chem.* **2002**, *39*, 1223–1240.